Radiology Case Reports 17 (2022) 1506–1511

Available online at www.sciencedirect.com

ScienceDirect

journal homepage: www.elsevier.com/locate/radcr

Case report

Nonfunctioning adrenal cortical carcinoma with skeletal muscle metastasis: Case report and imaging at limited resource center ☆,☆☆

Ramakrishna Narra, MD, DNB, DM[a,*], *Shaheen Syed, MBBS, MD*[b], *Nethula Sowjanya, MBBS, MD*[b], *Satyanarayana Veeragandham, MBBS, MD*[c]

[a] *Depatment of Radiodiagnosis, Katuri Medical College, Guntur, Andhra Pradesh, India, 522017*
[b] *Katuri Medical College, Guntur, Andhra Pradesh, India, 522017*
[c] *Depatment of Pathology, Katuri Medical College, Guntur, Andhra Pradesh, India, 522017*

ARTICLE INFO

Article history:
Received 10 January 2022
Revised 27 January 2022
Accepted 1 February 2022

Keywords:
Adrenal tumor
Adrenal cortical carcinoma
Computed tomography
Metastases
Skeletal muscle
Rare tumor

ABSTRACT

Adrenal cortical carcinoma (ACC) is a rare, aggressive endocrine malignancy with a reported incidence of 1.0-2.0 cases per million population and a poor prognosis due to metastatic spread. About 25% of cases of ACC present with metastases at the time of diagnosis. Metastatic spread of ACC commonly involves lungs, liver, kidney, peritoneum, lymph nodes, venous extension to the renal vein or inferior vena cava and bone. We report a case of a 47-year-old male with a nonfunctioning ACC with metastases to skeletal muscle (subscapularis, paraspinal, iliacus and gluteus maximus muscle) in addition to metastasis to the lung, which was not reported in the literature. Unfortunately, the patient expired prior to the surgery due to respiratory distress.

© 2022 The Authors. Published by Elsevier Inc. on behalf of University of Washington. This is an open access article under the CC BY-NC-ND license (http://creativecommons.org/licenses/by-nc-nd/4.0/)

Introduction

ACC is the second most aggressive endocrine malignant tumor with an incidence of 1-2 per million population per year [1] and has a poor prognosis in case of metastatic disease. ACC has female predominance (F:M = 1.5-2.5), with a bimodal age distribution, the first peak in childhood (5-20 years) and the second peak in adults (4th-5th decade) [2,3]. ACC can be classified as functioning (hormone–secreting) comprising 60% and whereas 40% are nonfunctioning (non-hormone secreting) tumors. Functioning tumors present with early symptoms like Cushing's syndrome, virilization or feminization, while nonfunctioning tumors are diagnosed late and incidentally during the course of investigating of other clinical issues [4]. The exact cause is undetermined; however, most of them are considered hereditary. CT is considered as modality of choice for detection and characterization of adrenal masses.

☆ Acknowledgments: There is no funding source.
☆☆ Competing interests: The authors have declared that no competing interests exist.
* Corresponding author.
E-mail address: narra.ramki29@gmail.Com (R. Narra).
https://doi.org/10.1016/j.radcr.2022.02.002
1930-0433/© 2022 The Authors. Published by Elsevier Inc. on behalf of University of Washington. This is an open access article under the CC BY-NC-ND license (http://creativecommons.org/licenses/by-nc-nd/4.0/)

Fig. 1 – Chest radiograph posteroanterior view demonstrating multiple well-defined radiopaque lesions of variable sizes in both the lungs and well-defined pleural based radiopaque lesions noted in the left lower hemithorax.

Case presentation

A 47-year-old male presented with a history of dry cough, shortness of breath, left lower chest pain for 10 days. He was a smoker and alcoholic. He had no remarkable past medical and family history for any illness or causative factor. He was vaccinated with first dose of Covaxin. On examination, blood pressure was 128/82 mm Hg, pulse rate was 80-85 beats/min and regular, and the temperature was 36.8°C. On local examination of the lung, decreased tactile fremitus was noted in the left infrascapular and infra-axillary regions. On auscultation, decreased breath sounds were noted in both lungs. Initial routine laboratory workup was done, and the values were within normal limits. Real time reverse transcriptase polymerase chain reaction was negative for COVID-19, Red blood cells $5.11 \times 10^6/\mu L$, Hematocrit 42.3%, White blood cells $11.0 \times 10^3/\mu L$, Neutrophils 62.1%, Platelet count $390 \times 10^3/\mu L$, Erythrocyte sedimentation rate 13 mm, Glucose 120 mg/dL, Creatinine 1.1 mg/dL, Uric acid 3.1 mg/dL, Albumin/globulin ratio 1:1. The patient was hospitalized for further care.

Chest radiograph PA (posteroanterior) view performed demonstrated multiple well-defined radioopaque lesions of variable sizes in both the lungs. Well, defined pleural based lesions were noted in the left lower hemithorax (Fig. 1).

Computed tomography (CT) scan chest performed demonstrated multiple well-defined hypodense and soft tissue density lesions in both lungs of variable sizes. Two pleural based soft tissue density lesions were noted in the left paraspinal region from D3 to D7 abutting the aorta and adjacent to the posterolateral part of the 3rd-5th rib (Fig. 2). Heterogenous soft tissue density lesions were noted in the left infraspinatus, left serratus anterior, left subscapularis muscle. A large, ill-defined, heterogeneous lesion with necrosis was noted in the left suprarenal region (within the imaging field).

On abdominal ultrasound, a large, ill-defined, heterogeneous lesion with necrosis and increased vascularity was noted in the left suprarenal region.

On further workup, a Contrast-enhanced CT abdomen was performed, which demonstrated a well-defined irregular heterogeneous lesion measuring appx. $8.4 \times 8.4 \times 8.0$ cm of (HU= +30 to +40) with central hypodense necrosis and

Fig. 2 – (A) Computer tomography scan (CT) of the chest coronal reformatted image in lung window demonstrating well-defined soft tissue density lesions and nodules in the bilateral lungs. (B) Coronal reformatted computer tomography chest image in lung window demonstrating mediastinal and pleural based soft tissue density lesions in the left hemithorax. (C) Axial reformatted computer tomography chest image in lung window demonstrating pleural based lesions in the left lower hemithorax. Note well-defined soft tissue density lesion in lower lobe (arrow).

tiny calcified speck noted in the left suprarenal region, and abutting the kidney inferiorly (Fig. 3). Left adrenal gland was not visualized separately and left renal cortical margins are visualized separately as visualized in the cortical nephrogram phase. The attenuation measurements of the lesion on the precontrast phase of the scan were +38 HU, +70 HU on the portal venous phase, and +60 HU in the delayed phase with an absolute percentage washout of 31.2% and a relative percentage washout of 14.2% respectively. The right adrenal gland appears normal. Few heterogeneous enhancing lesions were noted in the left iliacus muscle, left erector spinae muscle and underneath gluteus maximus muscle and left subscapular and infraspinatus muscle (Fig. 4). Homogenous enhancement was noted in the lung and mediastinal lesions. Based on the findings, a possibility of a malignant adrenal mass with metastasis as described was considered.

Due to limited resources in our center Positron emission tomography-computed tomography scan was not done, hence further work up for additional occult musculoskeletal lesions was limited in our study.

Fine needle core biopsy was performed under ultrasound guidance in the left adrenal mass lesion and the left paraspinal (erectorspinae) muscular lesion, which demonstrated clear cells nests as diffuse infiltrating sheets and intervening sclerosed stroma. Nuclear pleomorphism was noted within these cells (Fig. 5).

Hormonal workup of Serum cortisol (early morning) 13.2 μg/dL, Serum metanephrine 18 pg/mL, Serum aldosterone 0.32 ng/mL/h, renin activity and dexamethasone test were all within normal limits.

Based on the imaging workup, a diagnosis of ACC with metastatic spread was considered. Left adrenalectomy and palliative resection of the mass with further chemotherapy, radiotherapy was planned. Unfortunately, the patient expired due to respiratory distress prior to commencement of the treatment possibly due to metastatic disease. Autopsy was not done as the patients family members denied permission and did not give consent.

Discussion

ACC is the second most aggressive endocrine malignant tumor with an incidence of 1-2 per million population per year and has a poor prognosis in case of metastatic disease. ACC has female predominance (F:M = 1.5-2.5), with a bimodal age distribution, the first peak in childhood (5-20 years) and the second peak in adults (4th-5th decade).

Imaging plays an important role in the demonstration of the lesion and differentiation of benign from malignant lesions. In 2%-10% of cases, ACC is bilateral [5]. Imaging features indicative of adrenal malignancy are size >4 cm, rapid growth, heterogeneous morphology, irregular margins, central necrosis, haemorrhage, calcification, invasion into adjacent structures, and venous extension. A total of 70% of ACC are typically >6 cm and can measure up to 25 cm in size [6]. Metastasis can be local or systemic. Local metastasis tends to involve surrounding structures such as pancreas, spleen, liver, intestine, retroperitoneum, venous extension to inferior vena cava, lymphatic spread through regional and para-aortic lymph nodes. Systemic metastases occur most frequently in the lung (40%-80%), liver (40%-90%), bone (5%-20%), Inferior vena cava (9%-19%) and brain and skin (<5%) [6] whereas metastatic spread to skeletal muscle is very rare manifestation which is not yet mentioned in the literature.

On unenhanced CT, ACC appears large, ill-defined, heterogenous with HU >10 and areas of calcification and necrosis. On Contrast-enhanced CT, heterogenous enhancement prominent peripheral enhancement of the tumor, is noted due to central necrosis [7]. CECT is a definitive method for staging and identifying metastatic sites to liver, lung, bone, regional and para-aortic lymph nodes [8].

On Magnetic resonance imaging (MRI) T2-weighted images, in the presence of hemorrhage and necrosis, ACC appears to have heterogeneous signal intensity. MRI is also useful for assessment of tumor invasion into inferior vena cava and renal vein thrombosis.

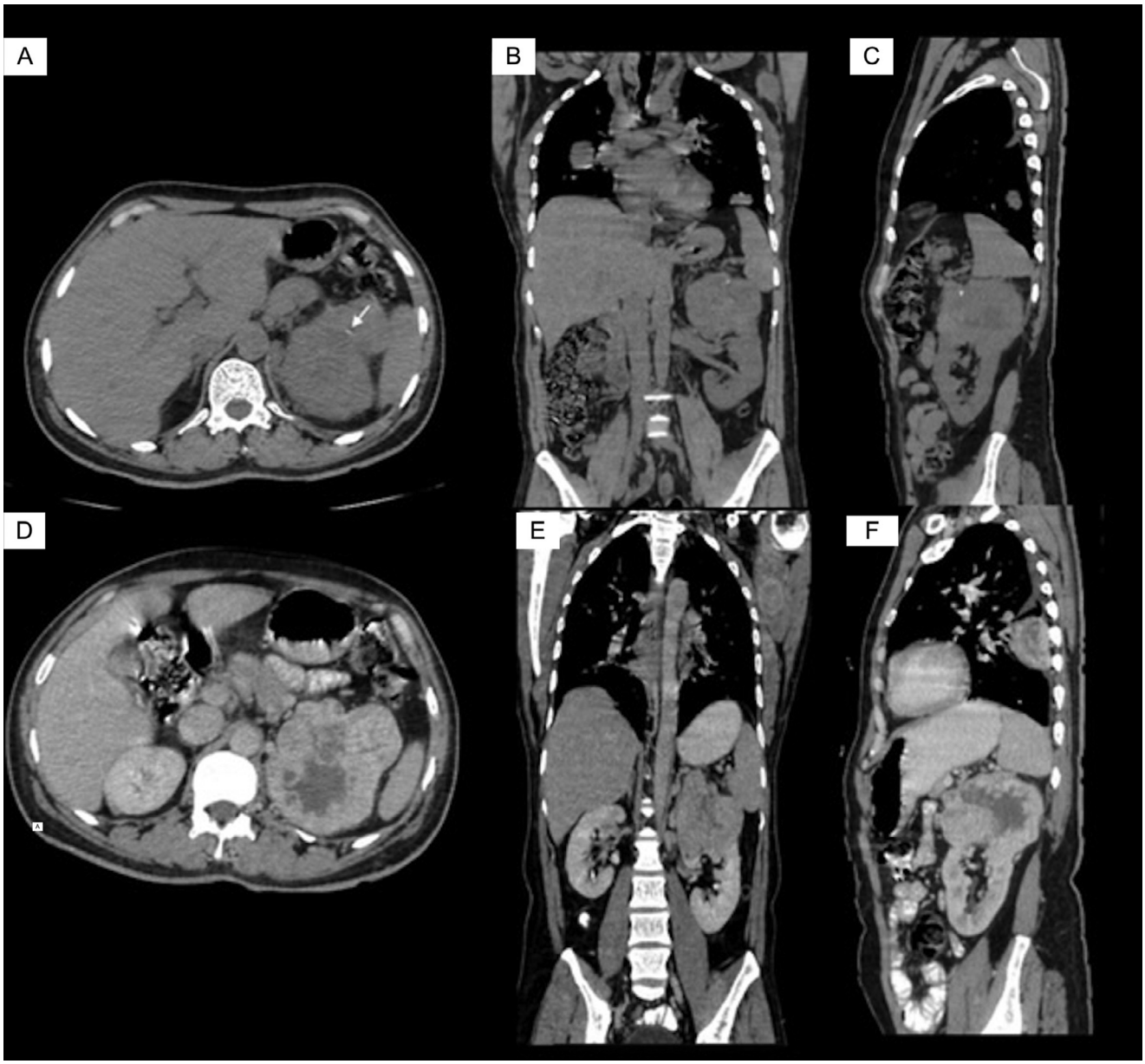

Fig. 3 – Axial, Coronal and Sagittal unenhanced (A–C) and enhanced computer tomography scan images (D–F) demonstrating the heterogeneously enhancing lesion in the left adrenal gland with areas of necrosis within. Few specks of calcification were noted within the mass (Fig. 3A) (arrow).

The histopathological study is used for assessing prognosis and also differentiate benign from malignant adrenal cortical tumors by Weiss score comprises of nine parameters by nuclear grading, mitotic rate of >5/50 HPFs, abnormal mitoses, ≥25% clear cells, >1/3 diffuse architecture, necrosis, venous invasion, sinusoidal invasion and capsular invasion [9].

The immunohistochemical study can be useful to distinguish ACC from other neoplasms such as pheochromocytoma and renal cell carcinoma. These tumors show positive for markers like vimentin, Melan A, synaptophysin, Neurofilament and α-inhibin overexpression. Negative for cytokeratin, chromogranin A [10].

[18 F] FDG Positron emission tomography is used as a diagnostic tool for differentiating benign from malignant lesions by using the cutoff value ratio of adrenal-to-liver max SUV (standardized uptake value) >1.45 [11] and for staging of the tumor with distant metastasis.

The differential diagnosis of ACC includes adrenal adenoma, pheocromocytoma, renal cell carcinomas and metastasis.

The survival rate for ACC with metastatic disease at the time of diagnosis is <1 year [12].

Fig. 4 – (A) Axial enhanced computer tomography scan image demonstrating heterogeneously enhancing soft tissue lesion in the left erector spinae muscle (arrow). (B) Axial enhanced computer tomography scan image demonstrating heterogeneously enhancing soft tissue lesion in the left iliacus muscle (arrow). (C) Axial enhanced computer tomography scan image demonstrating heterogeneously enhancing soft tissue lesion in the left subscapularis muscle, infraspinatus muscle.

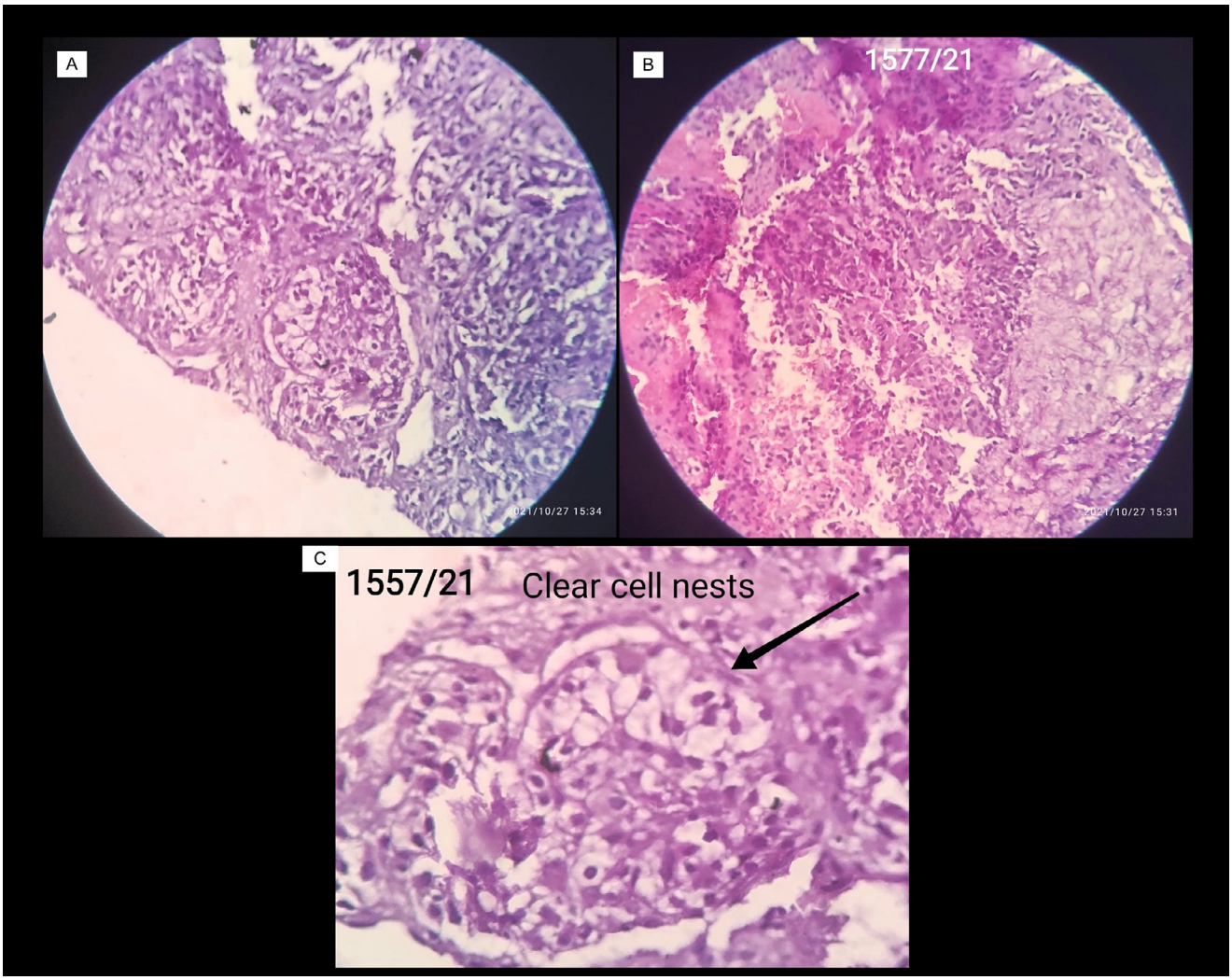

Fig. 5 – (A) Histopathological H and E image of core biopsy specimen from the adrenal lesion demonstrating clear cell nests as diffusely infiltrating sheets with intervening sclerosed stroma showing clear to eosinophilic cytoplasm with irregular nuclei and occasional inconspicuous nucleoli suggestive of adrenal cortical carcinoma. (B) Histopathological H and E image of core biopsy specimen from the left paraspinal metastatic lesion demonstrating clear cell nests and diffusely infiltrating sheets with intervening sclerosed stroma showing clear to eosinophilic cytoplasm. (C) Magnified H and E image demonstrating the described clear cell nests.

Patient Consent

Informed consent was obtained for the publication of this case report.

Contribution details

Collective work of all the authors in department of radiodiagnosis and pathology.

REFERENCES

[1] Almarzouq A, Asfar S, Hussain S, Al-Hunayan A, Aldousari S. Giant nonfunctioning adrenocortical carcinoma: a case report and review of the literature. BMC Res Notes 2014; 31:7.

[2] Luton JP, Cerdas S, Billaud L, et al. Clinical features of adrenocortical carcinoma, prognostic factors, and the effect of mitotane therapy. N Engl J Med 1990;322:1195–201 [PubMed] [Google Scholar].

[3] Bacalbasa N, Terzea D, Jianu V, Marcu M, Stoica C, Balescu I. Multiple visceral resections for giant non-secretory adrenocortical carcinoma in an elderly patient: a case report. Anticancer Res 2015;35(4):2169–74.

[4] Vassilopoulou-Sellin R, Schultz PN. Adrenocortical carcinoma. Clinical outcome at the end of the 20th century. Cancer 2001;92:1113.

[5] Latronico AC, Chrousos GP. Extensive personal experience: adrenocortical tumours. J Clin Endocrinol Metab 1997;82:1317–24.

[6] Fishman EK, Deutch BM, Hartman DS, Goldman SM, Zerhouni EA, Siegelman SS. Primary adrenocortical carcinoma: CT evaluation with clinical correlation. AJR 1987;148:531–5.

[7] Dunnick NR, Heaston D, Halvorsen R, Moore AV, Korobkin M. CT appearance of adrenal cortical carcinoma. J Comput Assist Tomogr 1982;6:978–82.

[8] Bharwani N, Rockall AG, Sahdev A, et al. Adrenocortical carcinoma: the range of appearances on CT and MRI. AJR Am J Roentgenol 2011;196:W706–14 [PubMed] [Google Scholar].

[9] Jain M, Kapoor S, Mishra A, Gupta S. Weiss criteria in large adrenocortical tumours: a validation study. Agarwal Indian J Pathol Microbiol 2010;53(2):222–6 [PubMed] [Ref list].

[10] Hesketh PJ, McCaffrey RP, Finkel HE, Larmon SS, Griffing GT, Melby JC. Cisplatin based treatment of adrenocortical carcinoma. Cancer Treat Rep 1987;71(2):222–4 [Pubmed].

[11] Groussin L, Bonardel G, Silvéra S, et al. 18F-fluorodeoxyglucose positron emission tomography for the diagnosis of adrenocortical tumours: a prospective study in 77 operated patients. J Clin Endocrinol Metab 2009;94(5):1713–22 Crossref, Medline, Google Scholar.

[12] Ayala-Ramirez M, Jasim S, Feng L, Ejaz S, Deniz F, Busaidy N, Waguespack SG, Naing A, Sircar K, Wood CG, Pagliaro L, Jimenez C, Vassilopoulou-Sellin R, Habra MA. Eur J Endocrinol 2013;169(6):891–9 [PubMed] [Ref list].